Hindawi Publishing Corporation
Journal of Nanomaterials
Volume 2011, Article ID 571601, 8 pages
doi:10.1155/2011/571601

Research Article

Fe-Doped TiO_2 Nanoparticles Produced via MOCVD: Synthesis, Characterization, and Photocatalytic Activity

Siti Hajar Othman,[1] Suraya Abdul Rashid,[1,2] Tinia Idaty Mohd Ghazi,[1] and Norhafizah Abdullah[1]

[1] *Department of Chemical and Environmental Engineering, Faculty of Engineering, University Putra Malaysia, Selangor, 43400 Serdang, Malaysia*
[2] *Advanced Materials and Nanotechnology Laboratory, Institute of Advanced Technology, University Putra Malaysia, Selangor, 43400 Serdang, Malaysia*

Correspondence should be addressed to Suraya Abdul Rashid, suraya@eng.upm.edu.my

Received 29 November 2010; Revised 15 February 2011; Accepted 20 February 2011

Academic Editor: Sherine Obare

Iron (Fe)-doped titanium dioxide (TiO_2) nanoparticles were produced via the metallorganic chemical vapour deposition (MOCVD) method at 700°C. Different amounts of ferrocene as the Fe dopant source (0.001–0.05 g) were introduced inside the reactor together with the titanium precursor in order to synthesize different Fe dopant concentrations of TiO_2 nanoparticles. Nitrogen (N_2) adsorption results showed that increasing the Fe dopant concentration caused a slight increase in the surface area of the nanoparticles due to the decrease in nanoparticle size. The UV-diffuse reflectance spectra demonstrated an absorption shift in Fe-doped TiO_2 nanoparticles to longer wavelengths, thus showing an enhancement of the absorption in the visible spectrum. Bandgap energy values determined from the UV-diffuse reflectance spectra data decreased with an increase in the Fe dopant concentrations. The photocatalytic activity of Fe-doped TiO_2 nanoparticles was investigated via degradation of methylene blue under UV and fluorescent light. It was found that Fe doping reduced the photocatalytic activity of the samples. Based on X-ray photoelectron spectroscopy (XPS) results, it is believed that this is due to the unfavourable location of Fe^{3+} inside the interior matrix of the TiO_2 nanoparticles rather than on the exterior surface, which would affect photocatalytic behaviour.

1. Introduction

One of the most widely used materials is titanium dioxide (TiO_2) and it is extensively used for various fields of application especially as a photocatalyst for self-cleaning [1], water treatment [2], antibacterial [3], and air purification [4]. Other than that, TiO_2 has also been used for sensors [5], solar energy conversion [6], and as an antiultraviolet (UV) agent [7]. TiO_2 offer the extra advantages of being low cost, having high photocatalytic activity, high stability, nontoxicity, hydrophilicity, and a high refractive index. Up to now, researchers have shown increasing interest in improving this material for more efficient usage.

TiO_2 with a bandgap energy of approximately 3.2 eV requires a UV light source such as sunlight to be photoactivated. The addition of a dopant such as iron (Fe) into TiO_2 has been proven by previous researchers to improve some of its properties. For example, Fe doping has been proven to improve the photocatalytic activity of TiO_2 [8]. It is generally accepted that the improvement in the photocatalytic activity of Fe-doped TiO_2 compared to undoped TiO_2 is due to the fact that Fe^{3+} ions can act as both hole and electron traps that enhances the lifetime of the electrons and holes and thus improves the photocatalytic activity of TiO_2. Furthermore, Fe doping could also encourage the TiO_2 nanoparticles to absorb light at a higher wavelength, and therefore it can potentially be used for indoor applications [9].

The two common crystal structures of TiO_2 nanoparticles exist in the anatase and rutile phases. Most studies have shown that anatase has a higher level of photocatalytic activity than rutile and that rutile is a very poor photocatalyst [10]. However, it is extensively accepted that the optimal

photocatalytic activity of TiO_2 is obtained with a mixture of anatase and a small percentage of rutile. The most common commercial TiO_2 nanoparticles, Degussa P25, consists of 75% anatase and 25% rutile and has a high photocatalytic efficiency that benefits from the mixed phase of anatase and rutile. Fe doping can help to promote phase transition from anatase to rutile [9, 11]. Fe doping can also promote phase transition from amorphous to anatase [11], which is significant since amorphous TiO_2 is not photoactive.

Many methods have been employed to produce TiO_2 such as sol gel [12], water in oil emulsion [13], hydrothermal synthesis [14], pulsed laser deposition [15], diffusion flame reactor [16], and metal organic chemical vapour deposition (MOCVD) [17]. Among these, MOCVD is a promising method because of the ease and simplicity of the process. Conventional steps in sample preparation such as drying, reduction, centrifuging, or hydrothermal processing can be eliminated. The control of particle size and size distribution of the TiO_2 nanoparticles can be easily accomplished by simply adjusting the MOCVD parameters such as the deposition temperature and the flow rate of the carrier gas. Moreover, dopants can be easily introduced into the reactor through a solid source, either separated from or mixed with the precursor making it possible to produce doped TiO_2 via a one step process. MOCVD reactor also has the prospect to be scaled up to industrial scale production levels.

To the best of our knowledge, no report has yet been published on the effects of Fe doping on the photocatalytic activity of TiO_2 nanoparticles produced using the MOCVD method. Only the works of Zhang et al. [9, 18] have produced Fe-doped TiO_2-coated photocatalysts on supported activated carbon by MOCVD, and the photocatalytic properties of the samples were studied via the degradation of methyl orange. Furthermore, the method used to produce the Fe-doped TiO_2 was slightly different. This current study synthesizes Fe-doped TiO_2 nanoparticles by mixing the dopant and the precursor while Zhang et al. introduced the dopant separated from the precursor; a codeposition method [18] as well as a one-step process [9]. Both methods by Zhang et al. produced Fe-doped TiO_2 coating that exhibited good photocatalytic activity under visible light irradiation.

In our previous work, we prepared the undoped and Fe-doped TiO_2 nanoparticles using the same reactor at deposition temperatures of 400 and 700°C [11]. We specifically studied the effect of Fe doping on the phase transition and the size of the TiO_2 nanoparticles produced. The aim of the present work is to investigate the effect of Fe doping on the surface area, light absorption, bandgap energy, and photocatalytic activity of the samples produced. The amount of Fe dopant was varied from 0.001 to 0.05 g in order to synthesize different concentrations of Fe-doped TiO_2 nanoparticles. The surface area and average nanoparticle size of the samples were studied using Nitrogen (N_2) adsorption, the light absorption and bandgap energy were determined using diffuse reflectance spectroscopy (DRS), and the chemical state of the particle surface was studied via X-ray photoelectron spectroscopy (XPS). The photocatalytic activity of the samples was studied via the degradation of methylene blue under the UV light and a fluorescent lamp.

2. Experimental

2.1. Synthesis of Undoped and Fe-Doped TiO_2 Nanoparticles. The titanium precursor, titanium (IV) butoxide (TBOT) from Sigma-Aldrich was used as received without further refinement. The precursor was stored in a bubbler located on a hot plate and maintained at 175°C to help it vaporize. Different amounts of Fe precursor which was ferrocene (0.001, 0.005, 0.01, 0.03, and 0.05 g) were mixed with 20 mL TBOT inside the bubbler to produce different Fe dopant concentrations. Nitrogen gas (400 mL/min) was used to purge the quartz tube during the initial heating step towards reaching the desired deposition temperature of 700°C after which, the precursor was introduced into the quartz tube using nitrogen as the carrier gas (400 mL/min) along with an oxygen feed (100 mL/min). Undoped and Fe-doped TiO_2 nanoparticles were then thermophoretically deposited inside the quartz tube upon thermal decomposition of the precursor vapour. After 3 hours, the reaction was terminated by switching off the nitrogen carrier gas and oxygen gas valves. The reactor was allowed to cool down to room temperature under a 400 mL/min nitrogen purge gas flow. The nanoparticle samples were collected from the wall of the quartz tube using a spatula and kept in a sealed container.

2.2. Characterization Method. UV-vis diffuse reflectance spectroscopy (DRS, Lambda 35, Perkin Elmer) was used to determine the light absorption of undoped and Fe-doped TiO_2 nanoparticles. The surface areas were determined by N_2 adsorption using the Brunauer-Emmett-Teller method (BET, Bel Japan Inc., Belsorp II). Before the measurement, all the samples were exposed to a vacuum condition at 150°C overnight to remove any remaining moisture. Finally, the chemical state (oxidation state and elemental composition) of the particle surface was studied by X-ray photoelectron spectroscopy (XPS, Omicron Nano Technology ELS 5000).

Note that in our previous work, initial characterization of the nanoparticles has already been reported [11]. Transmission electron microscope (TEM) was used to determine the nanoparticle size in terms of diameter as well as nanoparticle size distribution. X-ray diffraction (XRD) was employed to determine the phase of the samples, while energy dispersive X-ray (EDX) analysis was carried out to determine the elemental composition of the samples and to prove the presence of Fe in the TiO_2 crystal structure.

2.3. Photocatalytic Study. A simple photocatalytic reactor was used in this study similar to the setup described elsewhere [17]. The photocatalytic study was carried out at room temperature. A volume of 400 mL methylene blue with a concentration of 6 ppm (~pH 5.5) was poured into a 500 mL cylinder which was placed on a magnetic stirrer. An 8 W lamp (UV lamp—254 nm peak wavelength or a fluorescent lamp—420 nm peak wavelength, initial intensity 400 lumens) was immersed in the methylene blue. After that, 0.02 g of TiO_2 nanoparticles (isoelectric point ~pH 5.2) was introduced into the cylinder. The lamp and magnetic stirrer including an air pump (to provide air for the photocatalytic

Table 1: Effect of amount of Fe dopant on the surface area, average nanoparticle size, bandgap energy, and photocatalytic activity of TiO_2 nanoparticles produced via MOCVD including the commercial Degussa P25.

Amount of Fe dopant (g)	[a]Fe/Ti atomic ratio	[b]Surface area (m^2/g)	[c]Average nanoparticle size (nm)	Bandgap energy (eV)	[d]Rate constant under UV irradiation (h^{-1})	[d]Rate constant under fluorescent irradiation (h^{-1})
0	0	89.95	17.10	3.02	15.35	0.342
0.001	0.015	91.86	16.75	2.95	5.24	0.090
0.005	0.041	92.50	16.63	2.80	3.56	0.084
0.01	0.0107	95.55	16.10	2.60	3.07	0.078
0.03	0.0667	96.78	15.90	2.54	2.82	0.072
0.05	0.1317	113.19	13.59	2.00	1.40	0.042
0 (P25)	0	53.33	28.85	3.10	18.89	0.270

[a]Determined using EDX [11].
[b]Determined using BET method.
[c]Calculated using (1).
[d]Calculated using (2).

oxidation reaction) were switched on simultaneously. A volume of 6 mL of methylene blue suspension was then dispensed out every designated period of time. A UV-vis spectrophotometer (Thermo Scientific Helios Alpha) was used to determine the absorbance value at 664 nm (the absorbance peak of methylene blue). All experimental runs were repeated for at least 2 times.

3. Results and Discussions

3.1. Characterization. The surface areas of the undoped and Fe-doped TiO_2 nanoparticles were determined by N_2 adsorption using the BET method and tabulated in Table 1. The average nanoparticle size was also calculated from the BET data by applying the following equation:

$$D = \left(\frac{6}{\mathrm{SA} \times \rho}\right) \times 1000, \quad (1)$$

where D is the average nanoparticle size, SA is the surface area from the BET data, and ρ is the density taken as 3.9 g/cm^3. The results are also tabulated in Table 1.

It can be seen that there was a slight increase in the nanoparticle surface area from 91.86 to 113.19 m^2/g as the amount of Fe dopant was increased from 0.001 to 0.05 g. Accordingly, the average nanoparticle size was seen to slightly decrease with an increase in the Fe dopant concentration. The decrease in the average nanoparticle size can be ascribed to the fact that Fe doping slows the growth of the TiO_2 [19]. This is due to differences in the atomic radius of Fe^{3+} and Ti^{4+} which will result in some degree of lattice deformation when Fe^{3+} ions are incorporated into the crystal structure of TiO_2. The lattice deformation consequently causes the growth of grains to become restrained, leading to a decrease in the overall nanoparticle size [20]. These findings are supported by the XRD and TEM data previously reported [11]. Regardless of the deviation in the values determined from XRD and TEM, the results are consistent with the values determined from the BET method. The surface area and average nanoparticle size of the commercial TiO_2 nanoparticles, Degussa P25, are also tabulated in Table 1 whereby the values are significantly different in comparison with those of the samples produced.

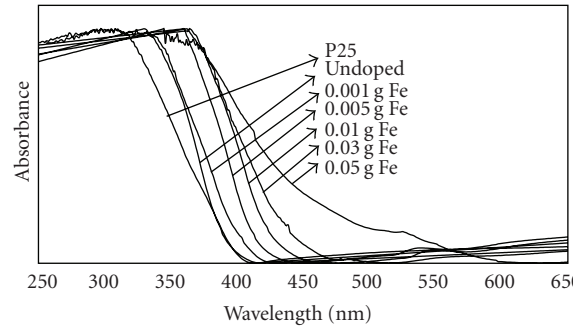

Figure 1: Diffuse reflectance spectra of undoped and Fe-doped TiO_2 nanoparticle samples including Degussa P25.

Diffuse reflectance spectroscopy was used to determine the absorption shift and the bandgap energy of all the samples. Figure 1 shows diffuse reflectance spectra of undoped and Fe-doped TiO_2 nanoparticles including the Degussa P25. As can be seen from Figure 1, Fe-doped TiO_2 samples show a strong absorption in the visible range, demonstrating a red shift in the band gap transition of the samples. The absorption shift to the higher wavelength became prominent as the concentration of Fe dopant was increased. However, undoped TiO_2 nanoparticles and Degussa P25 almost had no absorption above the fundamental absorption edge of 400 nm. These results seem to be consistent with the findings by Zhang et al. [18].

Figure 1 also shows that for samples obtained from relatively low concentrations of Fe dopant (<0.05 g Fe), no broad band centred at 500 nm was detected indicating that there were no separated phases of iron oxide [21]. However, a band at around 530 nm started to appear when the Fe dopant was increased to 0.05 g demonstrating the existence of separated phases of iron oxide. The results suggest that for samples containing relatively low concentration of Fe,

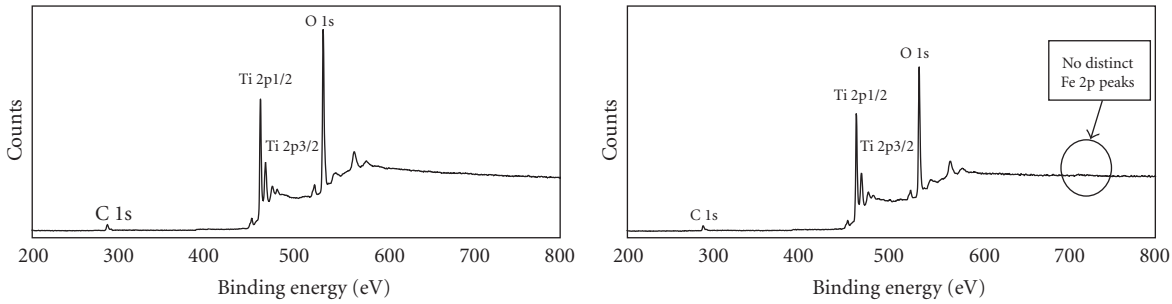

(a) Undoped TiO_2 (b) Fe-doped TiO_2 nanoparticles

Figure 2: XPS spectra of the synthesized undoped and TiO_2 nanoparticle samples.

the Fe was indeed incorporated inside the crystal lattice of the TiO_2 nanoparticles instead of forming iron oxide while high concentration of Fe dopant will lead to the formation of iron oxide. The presence of separated phases of iron oxide is not favored because it could decrease the photocatalytic activity of the samples [21].

A quantitative evaluation of the bandgap energy of all the samples can be determined by plotting $(a \cdot h\nu)^{1/2}$ against $h\nu$ (where a is absorbance and $h\nu$ is photon energy) and extrapolating the absorption edge to zero [22] (figure not shown). The bandgap energy values determined for all the samples are tabulated in Table 1. It can be clearly seen that the bandgap energy values decrease with an increase in the amount of Fe dopant, further supporting the red shifting in the band gap transition of the samples consistent with the findings of Gracia et al. [22]. The shift is attributed to the incorporation of the Fe ions into the TiO_2 crystal structure. It has been reported that red shifts of this type could be ascribed to the overlapping of the conduction bands due to Ti (d) of TiO_2 and the metal (d) orbital of the Fe ions which reduces the band gap energy of the TiO_2 and thus enabling them to absorb visible light [10].

XPS analysis was carried out in order to characterize the chemical state of the sample surface. Figure 2 shows the XPS spectra of the undoped and Fe-doped (0.03 g Fe) TiO_2 nanoparticle samples. The Fe-doped (0.03 g Fe) sample was chosen because this sample has an average amount of Fe/Ti ratio (atomic %) [11]. From Figure 2(a), a few apparent peaks located at binding energies of 285.4, 459.4, 465.2, 530.8, and 532.2 eV can be observed. The peak at a binding energy of 285.4 eV is assigned to the C 1s peak. The two peaks located at the binding energies of 459.4 and 465.2 eV correspond to the Ti 2p peak. The peaks for the pure Ti element are expected to appear at 455 (Ti 2p3/2) and 461 (Ti 2p1/2) eV [23]. There were shifts in the Ti 2p3/2 and Ti 2p1/2 peak positions due to the presence of tetravalent Ti^{4+}, as expected in TiO_2. On the other hand, the peaks at binding energies of 530.8 and 532.2 eV are assigned to the O 1s peak. Apart from the emission peaks of titanium (Ti), and oxygen (O), the peaks of carbon (C) were also observed most probably due to the carbon originating from the TBOT precursor used during sample preparation.

Meanwhile, for the XPS spectra of the doped sample, one would expect to see distinct Fe 2p characteristic peaks around a binding energy of 711 eV that should correspond to the presence of either Fe^{3+} or Fe^{2+} ions on the surface of the TiO_2 [8, 22]. Considering the ionic radius of Ti^{4+} (0.605 Å) and Fe^{3+} (0.645 Å) are almost the same, Fe^{3+} could replace Ti^{4+} when forming a solid solution. However, this was not the case since no Fe could be detected on the surface of the TiO_2 nanoparticles. Note that EDX results reported in previous work confirmed the presence of Fe in the samples [11]. Due to the lack of the aforementioned peaks, it is believed that the iron was most probably inserted into the interior matrix of the Fe-doped TiO_2 nanoparticles instead of the exterior surface [24, 25]. Furthermore, since XPS can only characterize the surface chemistry of the samples of up to approximately 5 nm while EDX can penetrate up to 5 μm depending on the instrument specification, the results obtained support this idea.

3.2. Photocatalytic Activity. Two types of light sources were used in the photocatalytic study to determine whether there was an enhancement in photocatalytic activity of the synthesized Fe-doped TiO_2 nanoparticles samples under UV and/or visible light irradiation. The photocatalytic activity of the samples was determined by the degradation of methylene blue aqueous solution over a period of 1 hour and 6 hours under UV light and fluorescent lamp irradiation, respectively. Under the UV light irradiation, the degradation of methylene blue occurred very quickly and was almost complete after only 10 minutes of reaction time. The photocatalytic activity for all the samples was quantitatively evaluated by calculating the respective pseudo first-order rate constants (k) according to the following equation:

$$\ln\left(\frac{C_o}{C}\right) = kt, \tag{2}$$

where C_o and C are, respectively, the initial concentration and the reaction concentration of methylene blue at time t. Figure 3 shows the plots of $\ln(C_o/C)$ against time for the undoped and Fe-doped samples including Degussa P25. The graphs were fitted with linear trendlines from which the rate constants were determined. Error bars represent the standard deviation values obtained from repeated experiments.

It can be seen from Figure 3 that all of the samples were capable of degrading methylene blue as indicated by the decrease in the methylene blue solution concentration throughout the period of the photocatalytic study. A very slight decrease of methylene blue for blank experiment is likely due to the interaction of methylene blue with light (photolysis). The rate constant represents the photocatalytic activity of the TiO_2 nanoparticle samples. The higher the rate constant value, the faster the degradation of methylene blue and thus the better the photocatalytic activity of the samples. For clarity, the rate constants obtained from the slope of the fitted linear trendlines are tabulated in Table 1.

Comparing photocatalytic activity of the undoped TiO_2 nanoparticles and the commercial Degussa P25, there are two important observations that can be deduced from the rate constant values tabulated in Table 1; undoped TiO_2 nanoparticles have a lower photocatalytic activity compared to Degussa P25 under UV light and conversely have a higher photocatalytic activity compared to Degussa P25 under fluorescent lamp. Firstly, since the undoped TiO_2 nanoparticles are purely anatase [11], Degussa P25 which consists of 75% anatase and 25% rutile has a higher photocatalytic activity that benefits from the mixed phase of anatase and rutile although the surface area is smaller and the particles size is larger than the undoped TiO_2 nanoparticles. This finding suggests that crystallinity plays a more important role than particle size in determining the photocatalytic activity as supported by the work of Othman et al. [17].

Secondly, undoped TiO_2 nanoparticles have a higher photocatalytic activity than Degussa P25 under fluorescent light probably due to the fact that the bandgap energy of undoped TiO_2 nanoparticles is more suitable and closer to the wavelength of the lamp that was used in this study. The bandgap energy values obtained can be converted to wavelength using the following equation [26]:

$$\lambda\,(\text{nm}) = \frac{1240}{\text{band gap (eV)}}, \tag{3}$$

where λ is wavelength in nm. Using (3), the respective calculated wavelength for the undoped TiO_2 nanoparticles and Degussa P25 are 410.6 and 400.0 nm, respectively. The fluorescent lamp that was used in this study has the highest peak intensity at a wavelength of around 420 nm, which is relatively closer to the wavelength of the undoped TiO_2 nanoparticles. This finding implies that choosing a suitable wavelength of light is important in order for the TiO_2 to work efficiently as a photocatalyst. Other than that, undoped TiO_2 nanoparticles are smaller in size and have a larger surface area for photocatalysis to occur, resulting in an improved photocatalytic activity than Degussa P25.

Furthermore, from Table 1, it can be seen that the rate constant of the samples under UV light irradiation is much higher compared to the rate constant under fluorescent lamp irradiation. This is not surprising since the absorbance values for the TiO_2 samples are much lower in the visible light region as shown previously in Figure 1. What is surprising is that there is a significant difference in rate constant values for undoped and Fe-doped TiO_2 nanoparticles. There is an unexpected decrease from 15.35 to 5.24 h^{-1} (UV light) and especially from 0.342 to 0.09 h^{-1} (fluorescent lamp) in photocatalytic activity of the samples as 0.001 g Fe dopant was introduced into the TiO_2 nanoparticle samples. This implies that the addition of Fe dopant had significantly decreased the photocatalytic activity. The photocatalytic activity of the samples decreased from 5.24 to 1.40 h^{-1} (UV light) and from 0.09 to 0.042 h^{-1} (fluorescent lamp) as the amount of Fe dopant was increased from 0.001 g to 0.05 g suggesting that increasing the amount of Fe dopant had further reduced the photocatalytic activity of the samples.

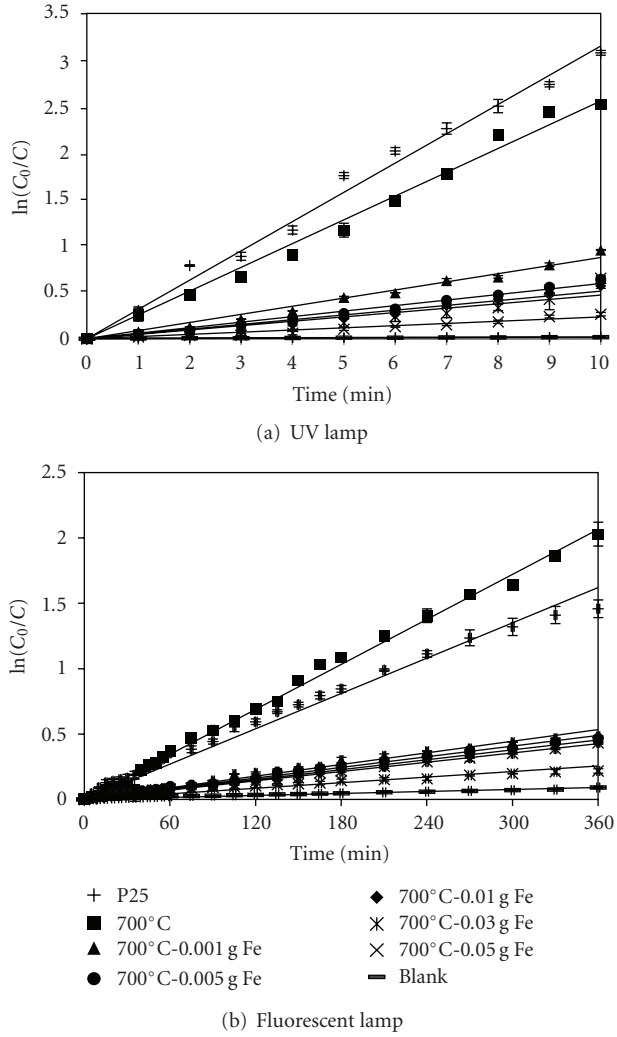

Figure 3: Photocatalytic activity for undoped and Fe-doped TiO_2 nanoparticle including Degussa P25 under (a) UV light illumination and (b) fluorescent lamp. Graphs were fitted with linear trendlines from which the rate constants were determined. Error bars represent the standard deviation values obtained from repeated experiments.

Under UV light irradiation, it is understandable that the addition of the Fe dopant had reduced the photocatalytic activity of the samples due to the fact that there was a decrease in bandgap energy or an extension of their absorption edge to the longer wavelength region as previously shown in Table 1 and Figure 1. This result is consistent with

the findings of Pal et al. [27]. They reported that photocatalytic activity of Yb-doped TiO_2 nanoparticles under UV light decreased due to the extension of the absorption edge of the nanoparticles towards the longer wavelength region.

However, it is not entirely clear as to why the addition of Fe dopant caused a significant decrease in photocatalytic activity under fluorescent lamp irradiation, especially since the bandgap energy was reduced and the diffuse reflectance spectra shown earlier in Figure 1 suggested that there was strong absorption in the visible light region. Moreover, the BET data shown in Table 1 indicated an improvement in surface area and a decrease in particle size, which could have enhanced the photocatalytic activity.

These findings seem to contradict to a few of the previous reports in terms of advantages of Fe-doping on the photocatalytic activity of TiO_2. For example, Zhang et al. [9, 18] reported that Fe-doped TiO_2-coated photocatalyst prepared by the MOCVD method exhibited good photocatalytic activities for the degradation of methyl orange under visible light irradiation compared to undoped samples. It is noted that their method used to introduce the Fe dopant source was different from the current study. Zhou et al. [8] also reported that a small amount of Fe dopant in mesoporous TiO_2 powder prepared by the sol-gel method could enhance the photocatalytic activity of the samples under a 365 nm UV lamp irradiation.

Nonetheless, further search in the literature revealed the work of Li et al. [25] who produced Fe-doped TiO_2 nanoparticles via a modified hydrothermal process. They found that the photocatalytic activity of their synthesized Fe-doped TiO_2 nanoparticles decreased with the increase of the Fe content, consistent with the findings in this study. Furthermore, their XPS data indicated that the Fe was not located on the exterior of the samples but rather in the interior. These findings reveal that the location of the Fe in the crystal structure plays a major role in determining the photocatalytic properties of the doped samples.

It is generally accepted that the improvement in the photocatalytic activity of the Fe-doped TiO_2 compared to undoped TiO_2 is due to the fact that Fe^{3+} ions can act as both electron and hole traps that enhance the lifetime of the electrons and holes. Acting as both electron and hole traps, Fe^{3+} ions can translate into Fe^{2+} and Fe^{4+} ions by trapping photo-generated electrons and holes ((5) and (6)). Since Fe^{2+} and Fe^{4+} ions are relatively unstable in contrast to Fe^{3+} ions, the trapped charges can easily release from Fe^{2+} or Fe^{4+} ions and then migrate to the surface to initiate the photocatalytic reaction. Fe^{2+} ions can be oxidized to Fe^{3+} ions by transferring electrons to absorbed O_2 on the surface of TiO_2 (7) or a neighbouring surface of Ti^{4+} ions (8). The adsorbed O_2 is then reduced to O^{2-} ((7) and (9)), which can enhance the photocatalytic activity. Meanwhile, Fe^{4+} ions can be reduced to Fe^{3+} ions by releasing electrons in which the surface hydroxyl group turn into hydroxyl radical (10) that can further improve the photocatalytic activity [20]:

$$TiO_2 + h\nu \longrightarrow e^- + h^+ \quad (4)$$

$$Fe^{3+} + h^+ \longrightarrow Fe^{4+} \quad (5)$$

$$Fe^{3+} + e^- \longrightarrow Fe^{2+} \quad (6)$$

$$Fe^{2+} + O_2 \longrightarrow Fe^{3+} + O^{2-} \quad (7)$$

$$Fe^{2+} + Ti^{4+} \longrightarrow Fe^{3+} + Ti^{3+} \quad (8)$$

$$Ti^{3+} + O_2 \longrightarrow Ti^{4+} + O^{2-} \quad (9)$$

$$Fe^{4+} + OH^- \longrightarrow Fe^{3+} + OH^{\bullet} \quad (10)$$

However, as the Fe^{3+} was inserted into the matrix interior of the TiO_2 nanoparticles instead of the exterior, the role of the Fe^{3+} ions changed. The Fe^{3+} ions were isolated far from the surface, and this led to a lower possibility of transferring trapped charge carriers to the surface [24, 25]. Consequently, the Fe^{3+} ions were more likely to serve as recombination centres ((5), (6), and (11)–(13)) for the electron and hole pairs instead of trap sites for eventual charge transfer at the interface [24, 25]. This results in lower photocatalytic activity [20, 25]:

$$Fe^{4+} + e^- \longrightarrow Fe^{3+} \quad (11)$$

$$Fe^{2+} + h^+ \longrightarrow Fe^{3+} \quad (12)$$

$$Fe^{4+} + Fe^{2+} \longrightarrow 2Fe^{3+} \quad (13)$$

$$Fe^{4+} + Ti^{3+} \longrightarrow Fe^{3+} + Ti^{4+} \quad (14)$$

$$Fe^{2+} + OH^{\bullet} \longrightarrow Fe^{3+} + OH^- \quad (15)$$

It is noteworthy to evaluate how different ways of introducing dopant into the MOCVD reactor could easily affect the location of the dopant inside the TiO_2 and hence affect the photocatalytic activity of the samples. Previous studies by Zhang et al. have used two different ways of dopant introduction into the MOCVD; via codeposition method [18] and via a one-step process [9]. Both methods have successfully produced Fe-doped TiO_2 coatings that exhibited good photocatalytic activity under visible light irradiation. In the codeposition method, the TiO_2 was first deposited onto the activated carbon. The deposition of Fe was conducted using the same MOCVD method only after the deposition of TiO_2 was completed [18]. For the one-step process method, both the precursor and Fe dopant were introduced simultaneously inside the MOCVD reactor using two separate gas lines [9]. Note that even for the codeposition method, two separate gas lines were used for the precursor and dopant. This indicates that the chemicals will only meet and react inside the reactor for both methods. Thus, for both methods especially the codeposition method, the possibility of Fe to be uniformly distributed on the matrix exterior instead of inserted into matrix interior is much higher.

In contrast, the current study employed a procedure whereby the dopant and precursor were mixed and maintained at 175°C inside a bubbler before they were introduced into the MOCVD reactor simultaneously via a gas line. Note that the melting point of solid ferrocene is around 172°C. It is speculated that the liquid precursor and solid dopant that were mixed together and maintained at a temperature of 175°C would first react inside the bubbler to form

a complex compound before going into the reactor. When the vapour decomposed inside the reactor and began to form nanoparticles, there was a higher possibility of Fe to exist in the matrix interior rather than the exterior and thus altering its role as recombination sites rather than electron and hole traps.

Note that although Fe-doped TiO_2 have lower photocatalytic activity than undoped TiO_2 nanoparticles, the doped nanoparticles find use in certain applications especially as anti-UV agents in cosmetics, paints, or plastics. It is generally accepted that as an anti-UV agent, it is essential to degrade the photocatalytic activity of the TiO_2 nanoparticles because strong oxidation potentials of TiO_2 could accelerate photodegradation reaction of some organic elements in these products. Therefore, it can be deduced that the choice of method to produce the Fe-doped TiO_2 nanoparticles should be made in view of the photocatalytic performance and applications.

4. Conclusions

Undoped and Fe-doped TiO_2 nanoparticles were successfully synthesized via the MOCVD method using TBOT as precursor. The N_2 adsorption results revealed that surface area increased with an increase in Fe dopant concentration demonstrating a reduction in the average nanoparticle size of the samples. Diffuse reflectance spectra indicated an absorption shift of the Fe-doped TiO_2 nanoparticles to longer wavelengths, thus showing an enhancement in the absorption of the visible spectrum. Bandgap energy values calculated from diffuse reflectance data displayed a red shift in the band gap transition. The effects become more pronounced with the increase of Fe dopant concentration. However, it was found that the Fe doping decreased the photocatalytic activity of the samples. XPS data illustrated that Fe^{3+} was not found on the surface exterior of the TiO_2 nanoparticles, but instead was inserted into the matrix interior, which had a direct impact on the photocatalytic activity of the nanoparticles. Due to the reduction in photocatalytic activity, it is believed that Fe^{3+} ions were more likely to serve as recombination centres for the electron and hole pairs instead of trap sites for eventual charge transfer at the interface. It can be concluded that the choice of method to produce the Fe-doped TiO_2 nanoparticles should be made in view of the photocatalytic performance and applications.

Acknowledgment

This work was financially supported by the Fundamental Research Grant Scheme, University Putra Malaysia (Grant no. 5523426).

References

[1] J. O. Carneiro, V. Teixeira, A. Portinha et al., "Iron-doped photocatalytic TiO_2 sputtered coatings on plastics for self-cleaning applications," *Materials Science and Engineering B*, vol. 138, no. 2, pp. 144–150, 2007.

[2] H. Lachheb, E. Puzenat, A. Houas et al., "Photocatalytic degradation of various types of dyes (Alizarin S, Crocein Orange G, Methyl Red, Congo Red, Methylene Blue) in water by UV-irradiated titania," *Applied Catalysis B*, vol. 39, no. 1, pp. 75–90, 2002.

[3] H. Zhang, H. Liu, C. Mu, C. Qiu, and D. Wu, "Antibacterial properties of nanometer Fe^{3+}-TiO_2 thin films," in *Proceedings of 1st IEEE International Conference on Nano Micro Engineered and Molecular Systems*, pp. 955–958, 2006.

[4] H. Yu, K. Zhang, and C. Rossi, "Experimental study of the photocatalytic degradation of formaldehyde in indoor air using a nano-particulate titanium dioxide photocatalyst," *Indoor and Built Environment*, vol. 16, no. 6, pp. 529–537, 2007.

[5] R. Rella, J. Spadavecchia, M. G. Manera et al., "Acetone and ethanol solid-state gas sensors based on TiO_2 nanoparticles thin film deposited by matrix assisted pulsed laser evaporation," *Sensors and Actuators B*, vol. 127, no. 2, pp. 426–431, 2007.

[6] H. S. Jung, J. K. Lee, M. Nastasi et al., "Preparation of nanoporous MgO-coated TiO_2 nanoparticles and their application to the electrode of dye-sensitized solar cells," *Langmuir*, vol. 21, no. 23, pp. 10332–10335, 2005.

[7] M. R. Hoffmann, S. T. Martin, W. Choi, and D. W. Bahnemann, "Environmental applications of semiconductor photocatalysis," *Chemical Reviews*, vol. 95, no. 1, pp. 69–96, 1995.

[8] M. Zhou, J. Yu, B. Cheng, and H. Yu, "Preparation and photocatalytic activity of Fe-doped mesoporous titanium dioxide nanocrystalline photocatalysts," *Materials Chemistry and Physics*, vol. 93, no. 1, pp. 159–163, 2005.

[9] X. Zhang and L. Lei, "One step preparation of visible-light responsive Fe-TiO_2 coating photocatalysts by MOCVD," *Materials Letters*, vol. 62, no. 6-7, pp. 895–897, 2008.

[10] S. I. Nishimoto, B. Ohtani, H. Kajiwara, and T. Kagiya, "Correlation of the crystal structure of titanium dioxide prepared from titanium tetra-2-propoxide with the photocatalytic activity for redox reactions in aqueous propan-2-ol and silver salt solutions," *Journal of the Chemical Society, Faraday Transactions 1*, vol. 81, no. 1, pp. 61–68, 1985.

[11] S. H. Othman, S. Abdul Rashid, T. I. M. Ghazi, and N. Abdullah, "Effect of fe doping on phase transition of TiO_2 nanoparticles synthesized by MOCVD," *Journal of Applied Sciences*, vol. 10, no. 12, pp. 1044–1051, 2010.

[12] M. Pal, J. G. Serrano, P. Santiago, and U. Pal, "Size-controlled synthesis of spherical TiO_2 nanoparticles: morphology, crystallization, and phase transition," *Journal of Physical Chemistry C*, vol. 111, no. 1, pp. 96–102, 2007.

[13] Y. Mori, Y. Okastu, and Y. Tsujimoto, "Titanium dioxide nanoparticles produced in water-in-oil emulsion," *Journal of Nanoparticle Research*, vol. 3, no. 2-3, pp. 219–225, 2001.

[14] M. Wu, J. Long, A. Huang, Y. Luo, S. Feng, and R. Xu, "Microemulsion-mediated hydrothermal synthesis and characterization of nanosize rutile and anatase particles," *Langmuir*, vol. 15, no. 26, pp. 8822–8825, 1999.

[15] R. Paily, A. DasGupta, N. DasGupta et al., "Pulsed laser deposition of TiO_2 for MOS gate dielectric," *Applied Surface Science*, vol. 187, no. 3-4, pp. 297–304, 2002.

[16] H. D. Jang and S. K. Kim, "Controlled synthesis of titanium dioxide nanoparticles in a modified diffusion flame reactor," *Materials Research Bulletin*, vol. 36, no. 3-4, pp. 627–637, 2001.

[17] S. H. Othman, S. Abdul Rashid, T. I. Mohd Ghazi, and N. Abdullah, "Effect of postdeposition heat treatment on the crystallinity, size, and photocatalytic activity of TiO_2 nanoparticles produced via chemical vapour deposition,"

Journal of Nanomaterials, vol. 2010, Article ID 512785, 10 pages, 2010.

[18] X. Zhang, M. Zhou, and L. Lei, "Co-deposition of photocatalytic Fe doped TiO_2 coatings by MOCVD," *Catalysis Communications*, vol. 7, no. 7, pp. 427–431, 2006.

[19] K. Naeem and F. Ouyang, "Preparation of Fe^{3+}-doped TiO_2 nanoparticles and its photocatalytic activity under UV light," *Physica B*, vol. 405, no. 1, pp. 221–226, 2010.

[20] T. Tong, J. Zhang, B. Tian, F. Chen, and D. He, "Preparation of Fe^{3+}-doped TiO_2 catalysts by controlled hydrolysis of titanium alkoxide and study on their photocatalytic activity for methyl orange degradation," *Journal of Hazardous Materials*, vol. 155, no. 3, pp. 572–579, 2008.

[21] J. A. Navio, G. Colon, M. I. Litter, and G. N. Bianco, "Synthesis, characterization and photocatalytic properties of iron-doped titania semiconductors prepared from TiO_2 and iron (III) acetylacetonate," *Journal of Molecular Catalysis A*, vol. 106, no. 3, pp. 267–276, 1996.

[22] F. Gracia, J. P. Holgado, F. Yubero, and A. R. Gonza'lez-Elipe, "Phase mixing in Fe/TiO_2 thin films prepared by ion beam-induced chemical vapour deposition: optical and structural properties," *Surface and Coatings Technology*, vol. 158-159, pp. 552–557, 2002.

[23] W. Li, S. Ismat Shah, C. P. Huang, O. Jung, and C. Ni, "Metallorganic chemical vapor deposition and characterization of TiO_2 nanoparticles," *Materials Science and Engineering B*, vol. 96, no. 3, pp. 247–253, 2002.

[24] Z. Li, B. Hou, Y. Xu, D. Wu, and Y. Sun, "Studies of Fe-doped SiO_2/TiO_2 composite nanoparticles prepared by sol-gel-hydrothermal method," *Journal of Materials Science*, vol. 40, no. 15, pp. 3939–3943, 2005.

[25] Z. Li, W. Shen, W. He, and X. Zu, "Effect of Fe-doped TiO_2 nanoparticle derived from modified hydrothermal process on the photocatalytic degradation performance on methylene blue," *Journal of Hazardous Materials*, vol. 155, no. 3, pp. 590–594, 2008.

[26] C. T. Hsieh, W. S. Fan, W. Y. Chen, and J. Y. Lin, "Adsorption and visible-light-derived photocatalytic kinetics of organic dye on Co-doped titania nanotubes prepared by hydrothermal synthesis," *Separation and Purification Technology*, vol. 67, no. 3, pp. 312–318, 2009.

[27] M. Pal, U. Pal, R. Silva Gonzalez, E. Sanchez Mora, and P. Santiago, "Synthesis and photocatalytic activity of Yb doped TiO_2 nanoparticles under visible light," *Journal of Nano Research*, vol. 5, no. 1, pp. 193–200, 2009.